Journal of Thermal Analysis and Calorimetry (2024) 149:5741–5754
https://doi.org/10.1007/s10973-024-13101-y

Experimentation with different alumina hybrid (50:50) suspensions as coolant on plate heat exchanger performance

Atul Bhattad[1]

Received: 9 October 2023 / Accepted: 16 March 2024 / Published online: 12 April 2024

Abstract

Energy evaluation of the plate heat exchanger is done using Al_2O_3 mixed hybrid nanofluids as a coolant. The various hybrid nanofluids (AlN–Al_2O_3, SiC–Al_2O_3, and MgO–Al_2O_3) with equal nanoparticle ratio (5:5) and Al_2O_3 (10:0) of 0.01% total volume concentration and DI water act as a coolant. The impact of different nanoparticle combinations, flow rate, and inlet temperature on the heat transfer rate, pump work, performance index, heat transfer coefficient, and effectiveness is examined. It is observed that the heat transfer rate, convective heat transfer coefficient, effectiveness, and performance index enhance with an increase in the flow rate and with the addition of nanoparticles. The heat transfer rate and heat transfer coefficient improve the maximum for SiC–Al_2O_3 hybrid nanofluid to 3.8% and 11.7%, respectively. In contrast, pump work enhances up to 0.25% for Al_2O_3 (10:0) nanofluid. The effectiveness and performance index improve up to 3.9% for SiC (5:5) hybrid nanofluid. Further, a correlation to estimate the Nusselt number of base fluid has been proposed for the studied cases.

Keywords Hybrid nanofluid · Heat transfer rate · Plate heat exchanger · Heat transfer coefficient · Coolant · Effectiveness

List of symbols

A	Effective area [m^2]
b	Channel spacing [m]
c_p	Specific heat [J kg^{-1} K^{-1}]
k	Thermal conductivity [W K^{-1} m^{-1}]
$\dot{m}$	Mass flow rate [kg s^{-1}]
Nu	Nusselt number [Dimensionless]
p	Pressure [pa]
Pr	Prandtl number [Dimensionless]
Q	Heat transfer rate [W]
Re	Reynolds number [Dimensionless]
t	Thickness [m]
T	Temperature [K]
U	Overall heat transfer coefficient [W K^{-1} m^{-2}]
W_{pump}	Pump work [W]
v	Volume concentration [%]
v	Velocity [m s^{-1}]
x	Volume of Al_2O_3 nanoparticle
X	Uncertainty [%]
y	Volume of second nanoparticle

✉ Atul Bhattad
atul45007@gmail.com

[1] Department of Mechanical Engineering, Koneru Lakshmaiah Educational Foundation, Vaddeswaram, AP 522502, India

Greek letters

α	Heat transfer coefficient [W K^{-1} m^{-2}]
ε	Effectiveness [Dimensionless]
μ	Dynamic viscosity [Pa s]
Ω	Volumetric flow rate [m^3 s^{-1}]
ρ	Density [kg m^{-3}

Abbreviations

Al_2O_3	Alumina particles
AlN	Aluminum nitride
DI	De-ionized water
HEX	Heat exchanger
HTC	Heat transfer coefficient [W K^{-1} m^{-2}]
HyNf	Hybrid nanofluid
LMTD	Log mean temperature difference [K]
MgO	Magnesium oxide
MWCNT	Multi-walled carbon nanotube
PHE	Plate heat exchanger
PI	Performance index [Dimensionless]
SEM	Scanning electron microscopy
SiC	Silicon carbide

Subscripts

bf	Base fluid
c	Cold
h	Hot
i	Inlet
nf	Nanofluid

o Outlet
w Wall

Introduction

Due to the power calamity, heat exchanger design and liquid characteristics need more surveys. Therefore, researchers studied it [1–13]. Authors used nanoparticle mixed working fluid as a sustainable solution to tackle an energy crisis and to enhance the performance of the heat exchanger for solar applications [14–18]. Pandey and Nema [19] used alumina–water coolant in a corrugated plate heat exchanger (PHE) for heat transfer and pressure loss analysis. The results showed that heat transfer features increased with the Reynolds number (Re) and decreased with particle concentration (v%). Javadi et al. [20] studied a plate heat exchanger's heat transfer and pressure loss with nanofluids. Providing grooves in the plate increases the performance of PHE [21]. Mansory et al. [22] tried to investigate the heat transfer of alumina–water nanofluid in the heat exchanger (HEX).

Using hybrid nanofluids [23–28] instead of primary liquids can improve the thermal performance of thermal devices because their properties can be tuned for different applications. Huang et al. [29] increased the heat transfer coefficient and pressure loss using an MWCNT (multi-walled carbon nanotubes)–water and alumina–water nanofluid mixture in the plate HEX. Kumar et al. [30] analyzed different hot plates with MWCNT–water mixed nanofluids and found that at a concentration of 0.75% v in water, CeO_2–MWCNTs could reduce exergy loss by 24.75%. Kumar et al. [31] studied hot plate heat transfer at different plate temperatures using different nanofluids and Cu–Al_2O_3/water mixed nanofluids. The combination of 5 mm plate spacing and MWCNT/water nanofluids performs best. MWCNT/water hybrid nanofluids (HyNf) in PHEs have been studied and shown to increase thermal performance [32, 33]. Bhattad et al. [34] evaluated the impact of individual particle volume ratio for the Al_2O_3–MWCNT/water hybrid mixture and found that the MWCNT nanofluid performs best. Bhattad et al. [35] considered different hybrid nanofluids in 0.1 v% concentration and found that the Al_2O_3–SiC combination is best in energy characteristics. Sokhal et al. [36] conducted experiments on an Al_2O_3 and CuO hybrid nano-doped liquid in a PHE. Changes in Re, temperature, and nanoparticle concentration measure performance. Adding nanoparticles enhanced the heat transfer rate (21%). Bhattad et al. [37–39] utilized hybrid nanofluids in PHE to investigate the energy, exergy, and cost performance at low temperatures and observed an enhancement

Table 1 Comparative investigation in the relevant field

Author/year	Operating variables	Nanofluid characteristics	Findings
Kumar et al. (2016) [30]	Nanofluid as coolant, $T_{ci}=20$ °C, $T_{hi}=50$ °C, $\Omega_c=\Omega_h=3$ lpm	Al_2O_3 + MWCNT, TiO_2 + MWCNT, ZnO + MWCNT, CeO_2 + MWCNT/water, (0.25–2.0 vol%)	Exergy loss was reduced by 24.75%
Kumar et al. (2016) [31]	Nanofluid as coolant, $T_{ci}=20$ °C, $T_{hi}=50$ °C, $\Omega_c=\Omega_h=3$ lpm, $b=2.5$–10.0 mm	Cu + Al_2O_3 hybrid nanofluid/DI/Water, (0.5–2.0 v%), Surfactant: CTAB	The least exergy loss and highest exergetic efficiency were found for 5 mm spacing at 0.75 v%
Kumar et al. (2016) [32]	Nanofluid as coolant, $T_{ci}=293$ K, $T_{hi}=348$ K	TiO_2 + MWCNT/water, (0.0–1.5 vol%)	The discrete phase methodology agrees with the test results
Bhattad et al. (2020) [35]	Nanofluid cold side and water hot side. $\Omega_c=2.0$–4.0 lpm, $\Omega_h=3$ lpm, $T_{ci}=10$–25 °C	Al_2O_3–SiC, Al_2O_3–AlN, Al_2O_3–MgO, Al_2O_3–CuO and Al_2O_3–MWCNT/water (0.1 v%) in ratio 4:1	HTC enhances by 31.2% for Al_2O_3–MWCNT and Irreversibility enhances by 1.6% for Al_2O_3–CuO hybrid nanofluid
Goodarzi et al. (2015) [40]	Counter flow, Turbulent flow, Re = 2500–10000	MWCNT-GA, FMWCNT-Cys, FMWCNT-Ag/Water, (0.0–1.0 mass%)	The heat transfer rate and HTC increase
Huang et al. (2016) [41]	Hybrid on the hot side and water on the cold side. Re = 182–956, Pr = 5.5–8, Discharge (0–0.16 lps), $T_{hi}=28$ °C, $T_{ci}=14$ °C	Hybrid nanofluid: MWCNT/water (0.0111 v%) and Al_2O_3/water (1.89 v%) in a ratio 1:2.5	HTC increases with an insignificant rise in pumping power

in the exergy and energy performances. Table 1 shows the comparative study conducted till now in the related area.

With the best of the authors' knowledge, fewer efforts have been observed with hybrid nanofluids in the PHE with a *particular particle volume ratio*. Moreover, for low-temperature applications, the research is even less using hybrid nanofluids as coolant. In the available literature, most authors used MWCNT nanoparticles as the main nanoparticle, which is expensive. Hence, in this study, the author decided to work with Al_2O_3 nanoparticle as a center particle as it is readily available at a low price with more chemical stability. An attempt has been made to explore the effect of different alumina–water hybrid nanofluids (*Al_2O_3–SiC, Al_2O_3–AlN, Al_2O_3–MgO, in equal particle ratio*) as a *coolant* on the energetic performance of the plate heat exchanger. The hybrid nanofluid prepared was of 0.01 v% concentration. The low concentration has been selected to save the cost and get the payback period early. Effects of coolant flow rate and inlet temperature were investigated on heat transfer rate, heat transfer coefficient (HTC), pump operation, effectiveness, and performance index (PI).

Test facility and data reduction

Hybrid nanofluids are made following the process of Bhattad et al. [35]. HyNfs with different nanoparticle combinations at 0.01 v% and equal particle volume ratio (5:5) using a two-step method are prepared (Fig. 1). The nanoparticles were first characterized. The quantity of nanoparticles was measured with an electronic balance and then mixed with deionized water with a stirrer and ultrasonic generator (MJL Lab Equipment and Supplies Use, India) for stability and homogeneity. The Al_2O_3 nanofluids of 0.01 v% concentration were prepared, and then, various mixed nanofluids of 0.01 v% concentration

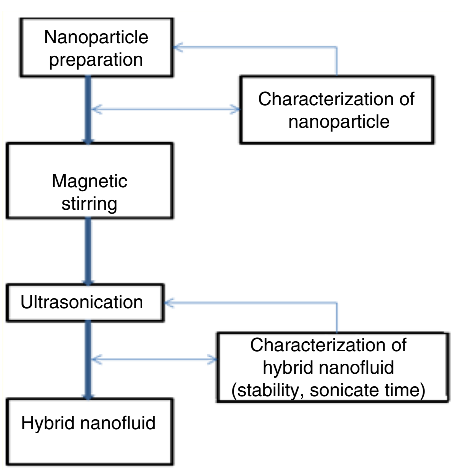

Fig. 1 Preparation method for hybrid nanofluid (Adapted from [34])

were prepared with the same steps. The stability test was performed by photographing the test tube, as shown in Fig. 2, and observed no sedimentation during the investigation for seven days, sufficient time to conduct the tests.

Scanning electron microscopy (SEM) was performed to confirm the particle size (Fig. 3). Particle size was observed at 115 nm (average size 45 nm) using ImageJ software. SEM image depicts that the particle is spherical, so in this case, the shape function is 1. Different DI water hybrid nanofluids (SiC–Al_2O_3, AlN–Al_2O_3, and MgO–Al_2O_3) with equal nanoparticle ratio (5:5), Al_2O_3 (10:0) of 0.01% total volume concentration, and DI water are used as a coolant. Detailed measurements of the examined heat exchanger are taken from Bhattad et al. [33]. The American KD2, thermal performance analyzer, measures conductivity and specific heat capacity. The viscosity is measured from the LVDV-II + Pro Brookfield digital viscometer. A digital weighing machine is utilized to measure the mass of the solution. The density was obtained from the expression $\rho = m/V$. Measurement of different thermal properties of the base liquid and other nano-sized particles at ambient temperature is listed in Table 2.

The present work is an extension work of the author, so the photograph of the test facility and operational process is adapted from Bhattad et al. [34]. As shown in Fig. 4, there are two flows (combined nanofluid and DI flow loop) for cold and hot fluid. The coolant circuit includes a constant temperature bath, a rotameter, and a pressure gauge. Here, nanofluids mixed with different types of Al_2O_3-deionized water are stored. An isothermal bath maintains the desired temperature. It then enters the heat exchanger through a flow meter. Install a control valve to change the flow of the nanofluid mixture. The hot cycle consists of an insulated water tank, a rotameter to record the flow, a differential manometer that records the pressure loss, and a centrifugal pump to deliver the hot liquid to the HEX. The temperature controller controls the required hot inlet temperature. Measure the temperature of the HyNf and hot water with inlet and outlet thermocouples. Test data help in determining heat transfer and pressure loss.

The data reduction and experimental validation procedure in energy measurement was the same as for Bhattad et al. [35]. This section provides some critical relationships.

Heat transfer rate is given by

$$Q = \dot{m}c_{\mathrm{p}}\Delta T \tag{1}$$

The overall heat transfer coefficient (U) is stipulated from

$$Q = U \cdot A \cdot \mathrm{LMTD} \tag{2}$$

where

$$\mathrm{LMTD} = \frac{T_{\mathrm{hi}} - T_{\mathrm{ho}} + T_{\mathrm{ci}} - T_{\mathrm{co}}}{\ln\left[\frac{(T_{\mathrm{hi}} - T_{\mathrm{co}})}{(T_{\mathrm{ho}} - T_{\mathrm{ci}})}\right]} \tag{3}$$

Fig. 2 Stability test

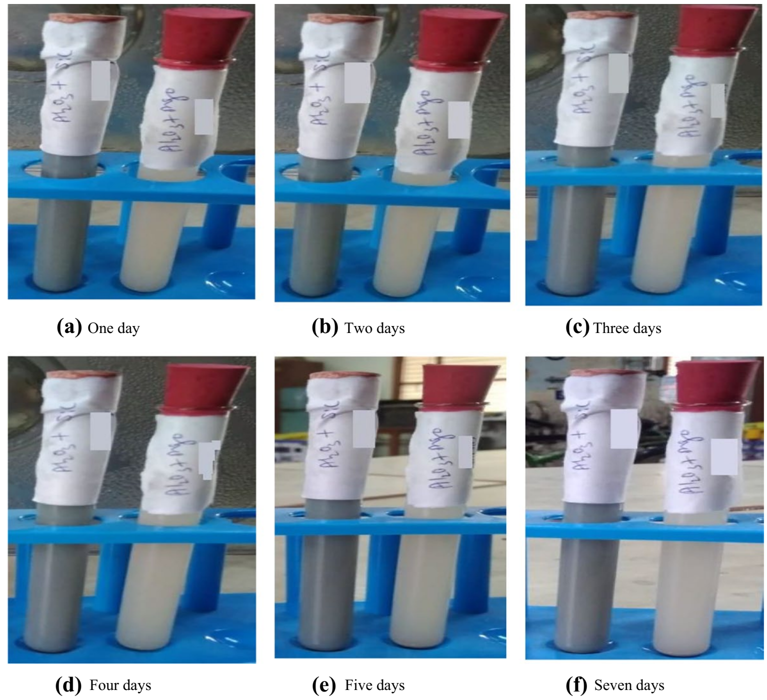

The cold side HTC (α_c) has been gathered from U, and the hot fluid HTC (α_h).

Fig. 3 SEM image of alumina–water nanofluid

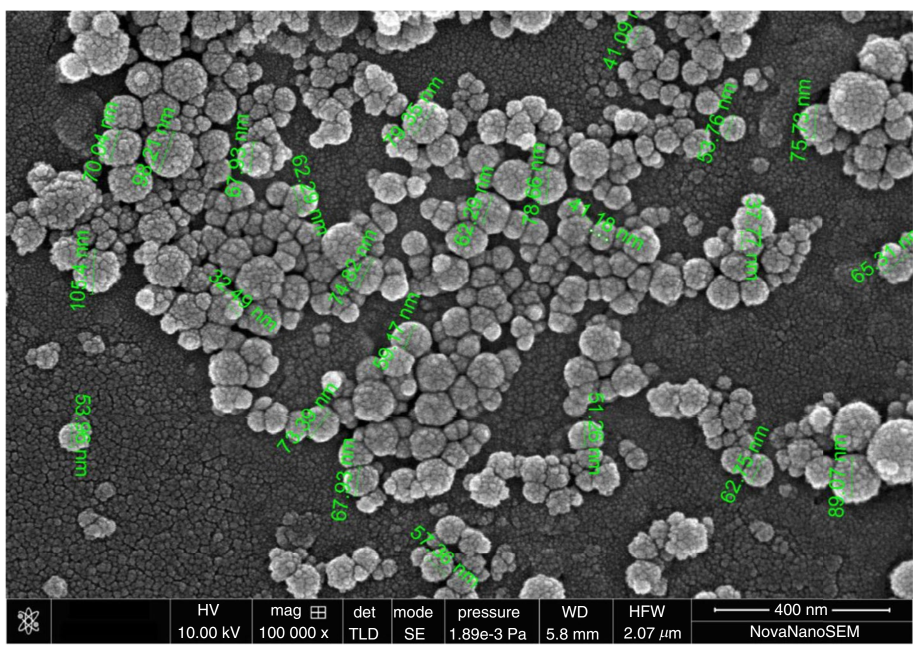

$$\frac{1}{\alpha_c} = \frac{1}{U} - \frac{t}{k_w} - \frac{1}{\alpha_h} \tag{4}$$

where k_w = Plate conductivity, (W m^{-1} K^{-1}), t = Plate thickness, (m).

Experimented U obtained with deionized water on both sides was compared with the estimated U acquired from available relationships from different authors [29, 41, 42], as shown in Fig. 5. Experimental data are inconsistent with the relationship. Thus, a new relationship is established for the thermal fluid Nusselt number. The liquid's heat transfer rate was found by approximating some Nusselt number

Table 2 Thermal properties of base fluid and nanoparticles at ambient temperature

Material	k/W m^{-1} K^{-1}	C_p/J kg^{-1} K^{-1}	ρ/kg m^{-3}	μ/Pa s
Alumina	40	773	3960	–
MgO	49	990	3580	–
SiC	350	1340	3220	–
AlN	285	740	3260	–
Water	0.6	4182	997	0.001003

equations. We think it complies with the power distribution law [35].

$$\mathrm{Nu} = a\mathrm{Re}^{b}\mathrm{Pr}^{c} \tag{5}$$

where the Nusselt number, Reynolds number, and Prandtl number are:

$$\mathrm{Nu} = \frac{\alpha D_{\mathrm{h}}}{k},\ \mathrm{Re} = \frac{\rho \cdot v \cdot d}{\mu},\ \text{and}\ \mathrm{Pr} = \frac{\mu c_{\mathrm{p}}}{k} \tag{6}$$

Hence,

$$\alpha = \frac{k \cdot a \cdot \mathrm{Re}^{\mathrm{b}}\,\mathrm{Pr}^{\mathrm{c}}}{D_{\mathrm{h}}} \tag{7}$$

where α is the heat transfer coefficient (W K^{-1} m^{-2}).

On combining Eqs. (4) and (7), we get Eq. (8)

$$\frac{1}{U} = \frac{1}{\frac{k_{\mathrm{h}} \cdot a \cdot \mathrm{Re}_{\mathrm{h}}^{\mathrm{b}}\,\mathrm{Pr}_{\mathrm{h}}^{\mathrm{c}}}{D_{\mathrm{h}}}} + \frac{1}{\frac{k_{\mathrm{c}} \cdot a \cdot \mathrm{Re}_{\mathrm{c}}^{\mathrm{b}}\,\mathrm{Pr}_{\mathrm{c}}^{\mathrm{c}}}{D_{\mathrm{h}}}} + \frac{t}{k_{\mathrm{w}}} \tag{8}$$

From available literature for Nu correlations, it was found that the exponent of Re varies between 0.5 and 1.0 and that of Pr varies between 0.3 and 0.5. Taking guess values between these ranges and doing many iterations, we obtained the most suitable values of a, b, and c as 0.235, 0.7, and 0.44. Hence, the proposed correlation in this investigation for DI water to calculate the heat transfer coefficient is given below as Eq. (9).

$$\mathrm{Nu} = 0.235\mathrm{Re}^{0.7}\mathrm{Pr}^{0.44}\ \left(R^2 = 0.94\right) \tag{9}$$

This relationship is valid for Reynolds numbers 100–400 and Prandtl numbers 4–7. HTC of the hot fluid (water) was obtained by combining Eqs. (4–9), and then, evaluate the

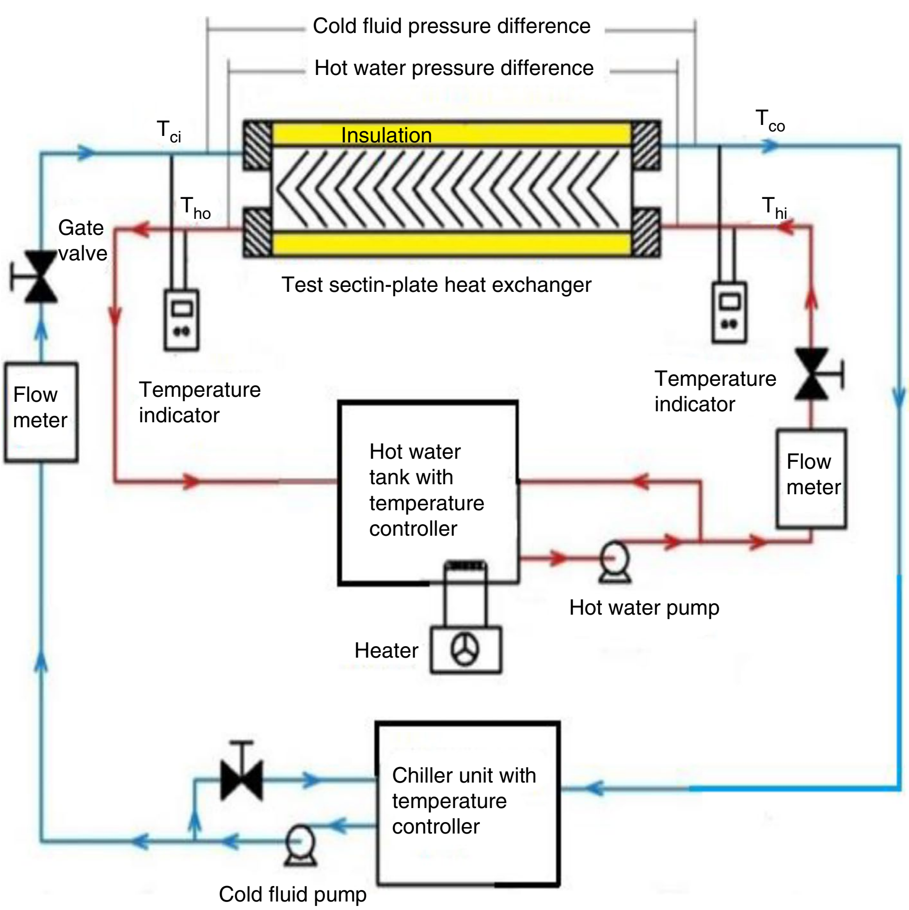

Fig. 4 Experimental setup (Adapted from [34])

Fig. 5 Comparison of estimated and tested U for DI water

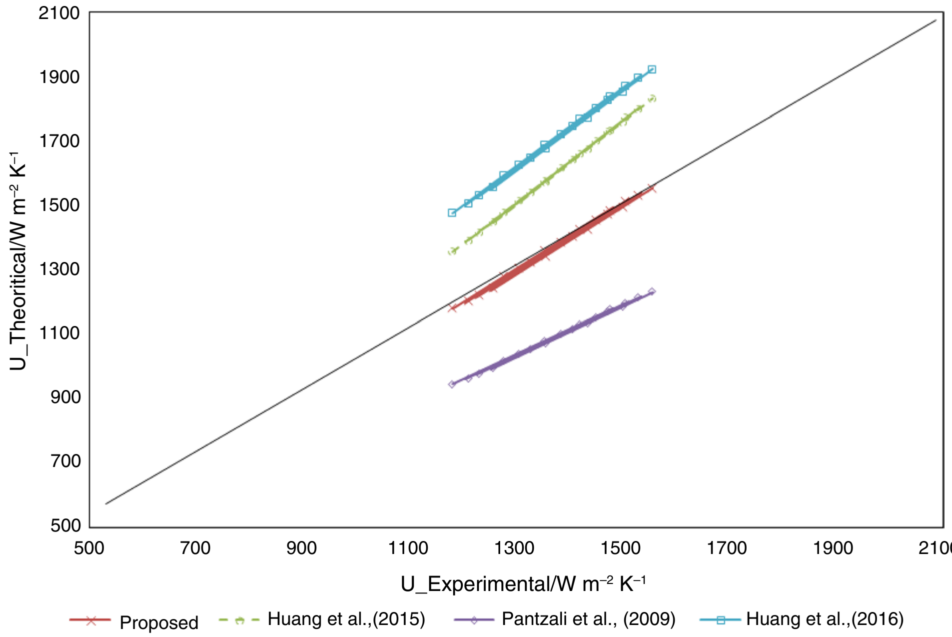

cold HTC by Eq. (4). Moreover, coolant pumping power has been calculated, assuming 20% pump efficiency [43], by

$$W_{\text{pump}} = \Delta p_c \dot{m}_c / 0.2\rho_c \tag{10}$$

The performance index (PI) is calculated as the fraction of the heat transfer rate and the pump power to measure the system's efficiency.

$$PI = Q/W_{\text{pump}} \tag{11}$$

Effectiveness (ε) is calculated by

$$\varepsilon = Q/(\dot{m}c_p)_{\min}(T_{\text{hi}} - T_{\text{ci}}) \tag{12}$$

Data for uncertainty study are presented in work by Bhattad et al. [34, 35]. Take uncertainty in each factor as x_n. The uncertainties of the dependent factor have been estimated from Eq. (13). Table 3 gives the predicted results' total uncertainty (X).

$$\frac{\delta X}{X} = \sqrt{\left[\left(\frac{\delta x_1}{x_1}\right)^2 + \left(\frac{\delta x_2}{x_2}\right)^2 + - - - - - + \left(\frac{\delta x_n}{x_n}\right)^2\right]} \tag{13}$$

Table 3 The uncertainties in the parameters

Variable	Uncertainty value/%
Cold and hot inward temperature	±0.2
Cold and hot outward temperature	±0.21
Cold and hot side flow rate	±2.5
Pressure drop	±2.3
Conductivity	±1.0
Viscosity	±1.0
Density	±1.0
Specific heat	±1.4
Q	4.5
Heat transfer coefficient	6.3
Pumping power	5.9
Performance index	7.2
Effectiveness	4.9

Results and discussion

Here, deionized water-based hybrid nanofluids at 0.01 v% concentration and equal particle ratio are considered as cold fluid and deionized water as hot fluid. The various effects of hybrid nanofluids were compared with base liquid (DI water), keeping the hot fluid flow at 3 lpm and hot-in temperature at 35 °C and altering cold-in flow (2.0–4.0 lpm in 0.5 increments) and inlet temperature (10–25 °C in 5 increments). The HyNf is nomenclature as x:y, where x indicates the volume of the Al_2O_3 nanoparticle and y indicates the volume of the other nanoparticle.

Impact of coolant flow rate

Variations with coolant flow at constant inlet temperature are shown in Figs. 6–10. In figures, notations 2, 2.5, 3, 3.5, and 4 represent the coolant flow rates in lpm. In addition, Al_2O_3 (10:0) represents DI water-based nanofluid containing

100% alumina nanoparticles, whereas SiC (5:5), AlN (5:5), and MgO (5:5) represent DI water-based hybrid nanofluid containing 50% alumina nanoparticles and 50% silicon carbide, aluminum nitride, and magnesium oxide nanoparticles, respectively. From Fig. 6, it has been found that the heat transfer rate increases with the coolant flow rate. The heat transfer rate varies with the temperature difference and the mass flow rate. Meanwhile, the flow rate of the liquid changes more than the temperature difference, so the temperature change increases. Due to the improved conductivity of the liquid (thermophoresis, Brownian motion, interaction, and collision of nanoparticles), the amount of heat changes due to the presence of nano-sized particles in the base liquid. The rise with the addition of nanoparticles is because of the variation in thermo-physical properties and a combination of distinct nanoparticles in a hybrid nanofluid. The relative movement between the nanoparticle and base fluid is the main reason behind this improvement that leads to the circulation of the nanoparticles due to the microconvection occurring by the movement of the fluid around the nanoparticles [35]. HyNfs are arranged in ascending order based on heat transfer rate: 100% alumina, 50% magnesium oxide, 50% aluminum nitride, and 50% silicon carbide. Alumina particles have contributed the rest of the 50%. It seems carbide is best for heat transfer rate (Q), followed by nitride and oxide. The HTC of the coolant rises with the flow rate and mixed nanofluids, as shown in Fig. 7. This enhancement is due to the augmentation in heat transfer rate with flow rate and the variation in thermal properties of various nanoparticles in HyNf. The order of the increment is similar to the heat transfer rate. SiC (5:5)/DI water mixture, a mixture of equal alumina and silicon carbide in DI water, depicts maximum enrichment in Q and HTC of around 2.4% and 11.4%, respectively.

As a disadvantage, pump work increases due to using hybrid nanofluids (Fig. 8). By adding nanoparticles, the viscosity and density of the primary liquid rise. Due to this dual phenomenon, pressure drops and pumping power increases [34]. Among the hybrid nanofluids, Al_2O_3 (10:0)/DI water mixture shows the maximum enhancement, and the SiC (5:5)/DI water combination shows the minimum enhancement in the required pump work. However, this variation is minimal due to less overall nanoparticle concentration and similar shape and size of nanoparticles. Also, the enhancement compared to base fluid is negligible (maximum 0.012%).

Factors like the effectiveness and performance index have been analyzed to visualize the impact of flow rate and nanoparticles on the heat exchanger performance. Figures 9–10 show that both the variables, effectiveness and PI, enhance by 2.4% with the rise in flow rate and dispersion of nanoparticles in the primary fluid. Nanoparticles in the fluid increase the temperature variation (comes in the numerator). In contrast, the inlet temperatures are fixed (comes in the denominator). Hence, the effectiveness increases with the application of nanoparticles.

Moreover, the increased performance index is the relative change in pump work and heat transfer rate. The

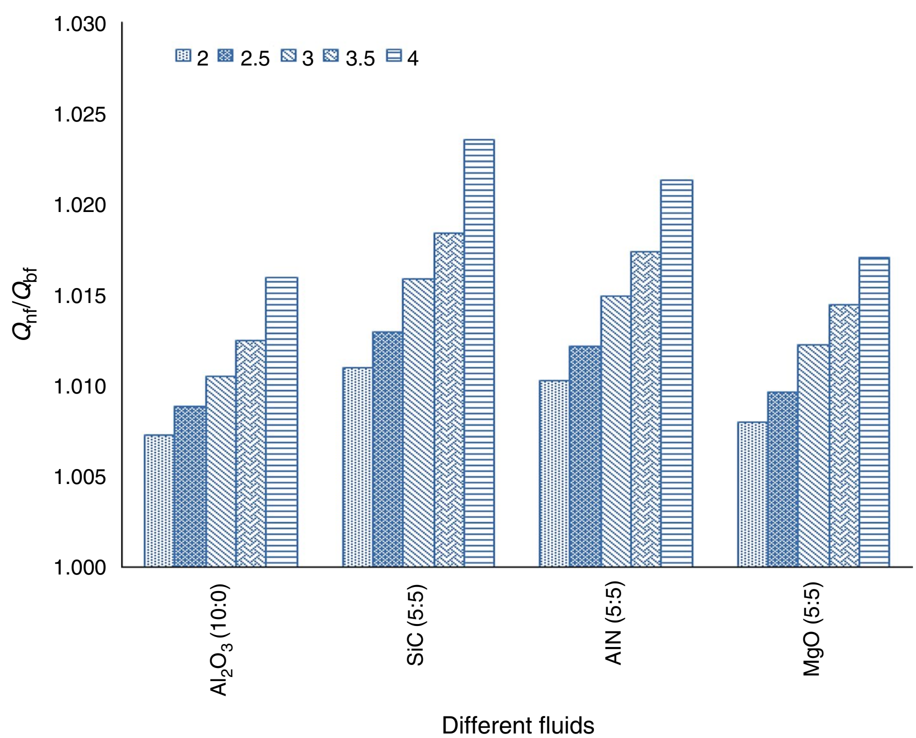

Fig. 6 Change in heat transfer rate with flow rate

Fig. 7 Change in heat transfer coefficient with flow rate

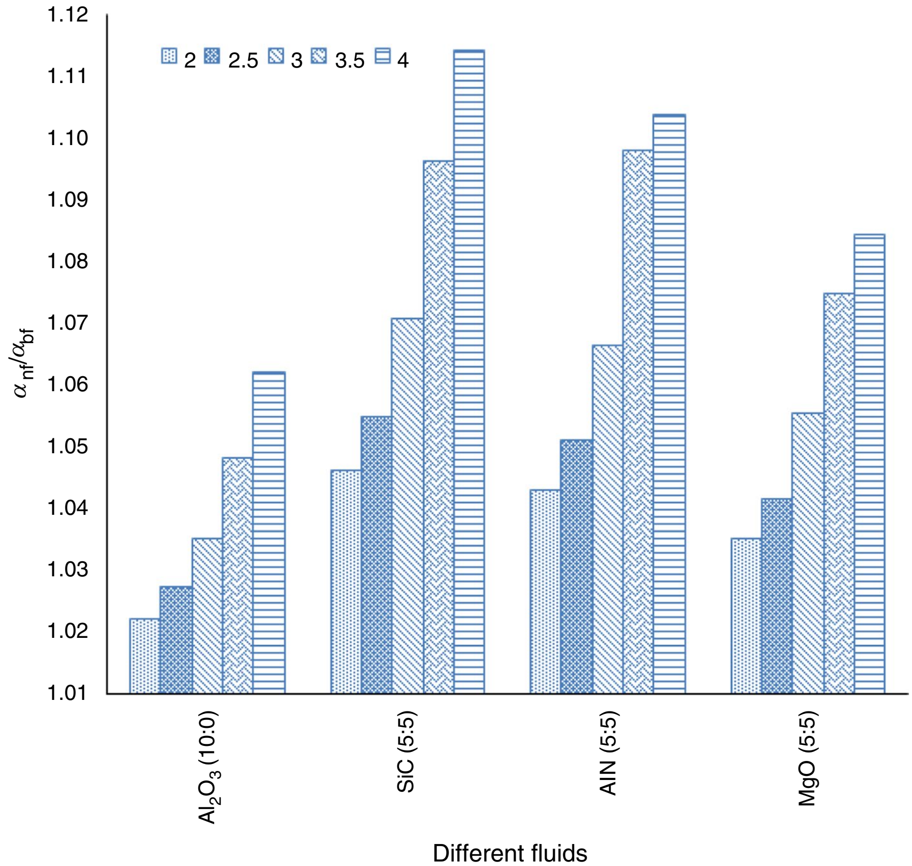

heat transfer rate enhances comparatively more than the pump work with the inclusion of nanoparticles. The order of enhancement, ascending order, in the performance index is as follows: alumina, magnesium oxide, aluminum nitride, and silicon carbide hybrid nanofluids. This enhancement is maximum for Al_2O_3–SiC (5:5)/DI water hybrid nanofluid and minimum for 100% Al_2O_3/DI water nanofluid.

Impact of coolant inlet temperature

Variations with coolant inlet temperature at a constant flow rate can be seen in Figs. 11–15. In figures, notations 10, 15, 20, and 25 represent the coolant inlet temperatures in degree Celsius (°C). In Fig. 11, the heat transfer rate declines with increasing cooling inlet temperature. The temperature difference decreases with an increasing coolant inlet temperature. Therefore, the amount of heat transferred will fall for a constant flow. Further, the heat transfer increased with hybrid nanofluids, and the most significant improvement (about 3.8%) was observed in SiC (5:5)/DI water hybrid nanofluids. Increasing coolant inlet temperature augments the convective HTC due to increased thermal conductivity and decreased viscosity. In comparison with the base fluid, the convective HTC of the HyNf increases, as shown in Fig. 12. The heat transfer coefficient ratio increases with an increase in inlet temperature of coolant because the mean temperature difference increases with increase in the temperature. This gives rise to the heat transfer coefficient. The HTC of SiC (5:5) mixed fluid is the best, with 11.7% enhancement.

Figure 13 shows the decrease in the pump work as the coolant inlet temperature increases. An increase in the temperature reduces the viscosity of the liquid; hence, the pressure drops, and the required energy consumption is reduced. With hybrid nanofluids, required pump work increases due to the increased pressure loss. It was observed maximum for the liquid containing the highest density nanoparticles. In this study, pumping power has been observed as maximum for Al_2O_3 (10:0) and minimum for SiC (5:5) hybrid nanofluids, respectively. Figures 14–15 show enhancement (around 3.9%) in the effectiveness and performance index with increased cold flow inlet temperature. Improvement has been found maximum for SiC (5:5) hybrid nanofluids and minimum for Al_2O_3 (10:0) nanofluids.

An enrichment in the heat transfer rate, HTC, effectiveness, and PI is found in a hybrid nanofluid. An insignificant rise in the pressure drop was observed for HyNfs due to less concentration of the nanoparticles. A correlation of Nusselt number has been proposed for hot fluid Eq. (9). The performance index of hybrid nanofluid is comparatively more

Fig. 8 Change in pump work with flow rate

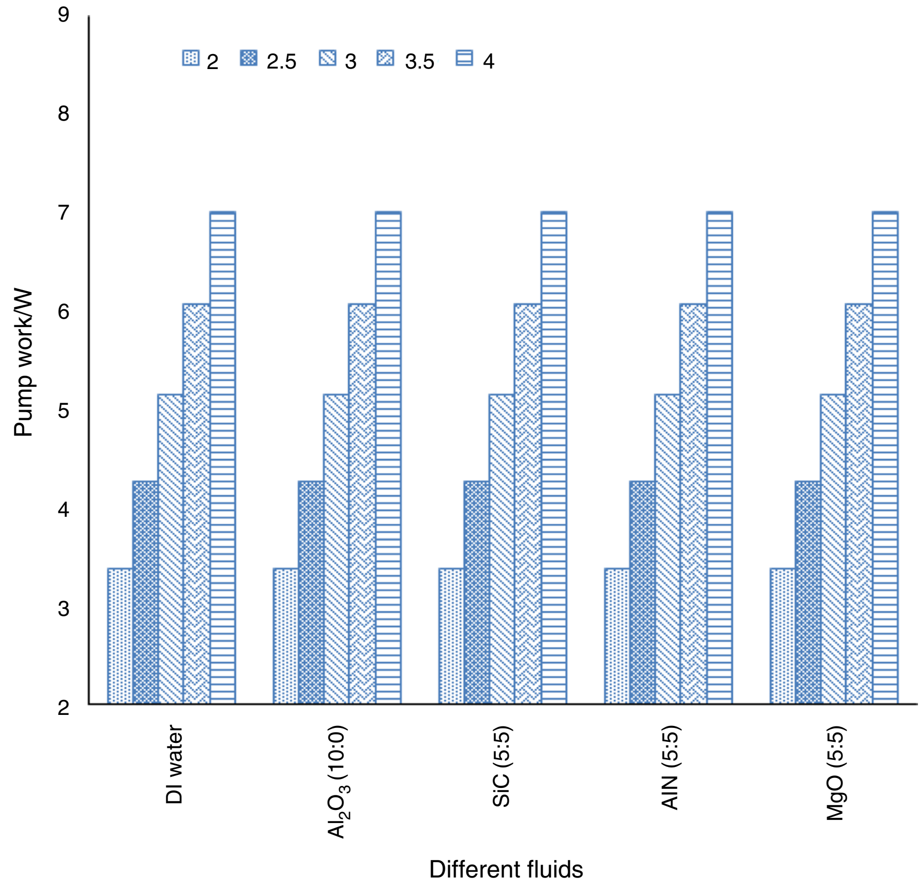

Fig. 9 Change in effectiveness with flow rate

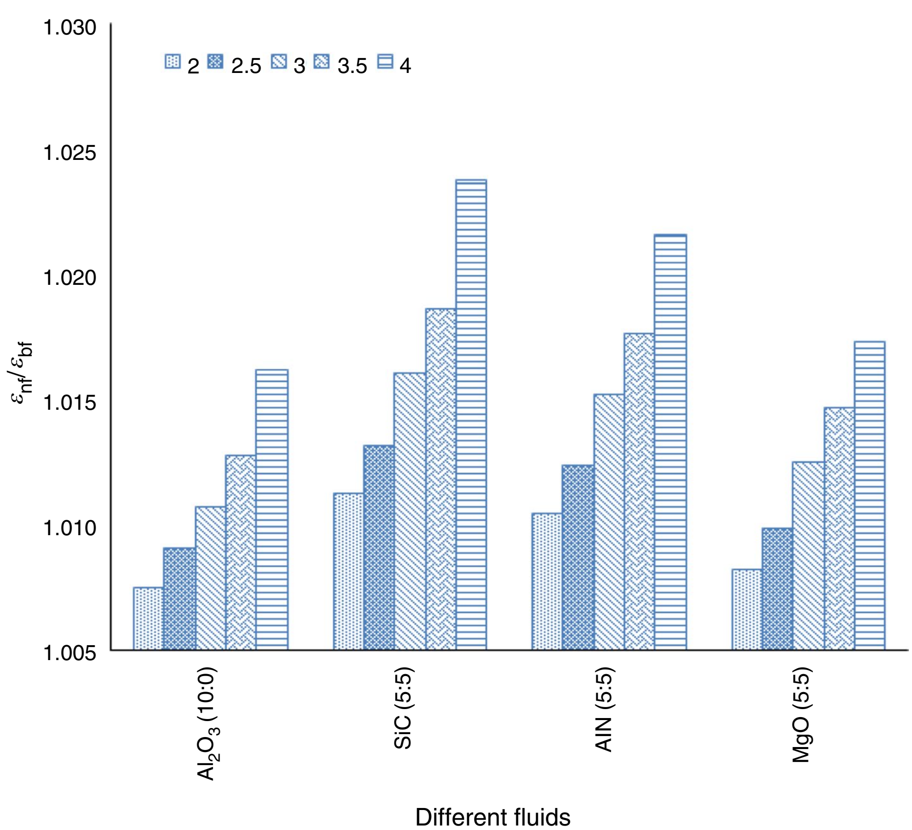

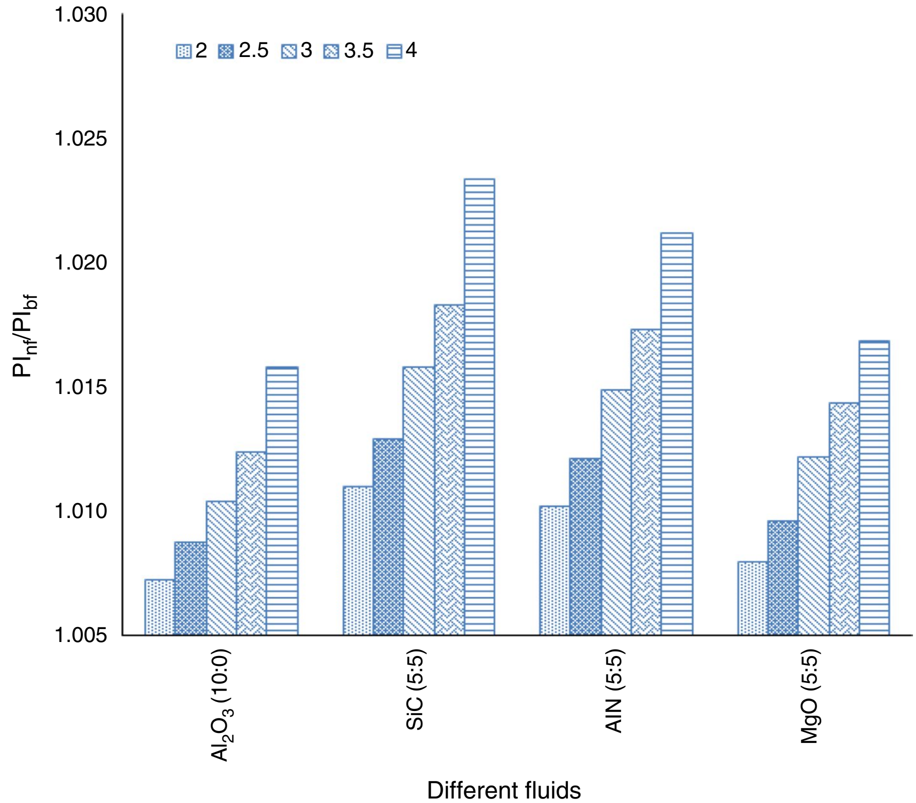

Fig. 10 Change in performance index with flow rate

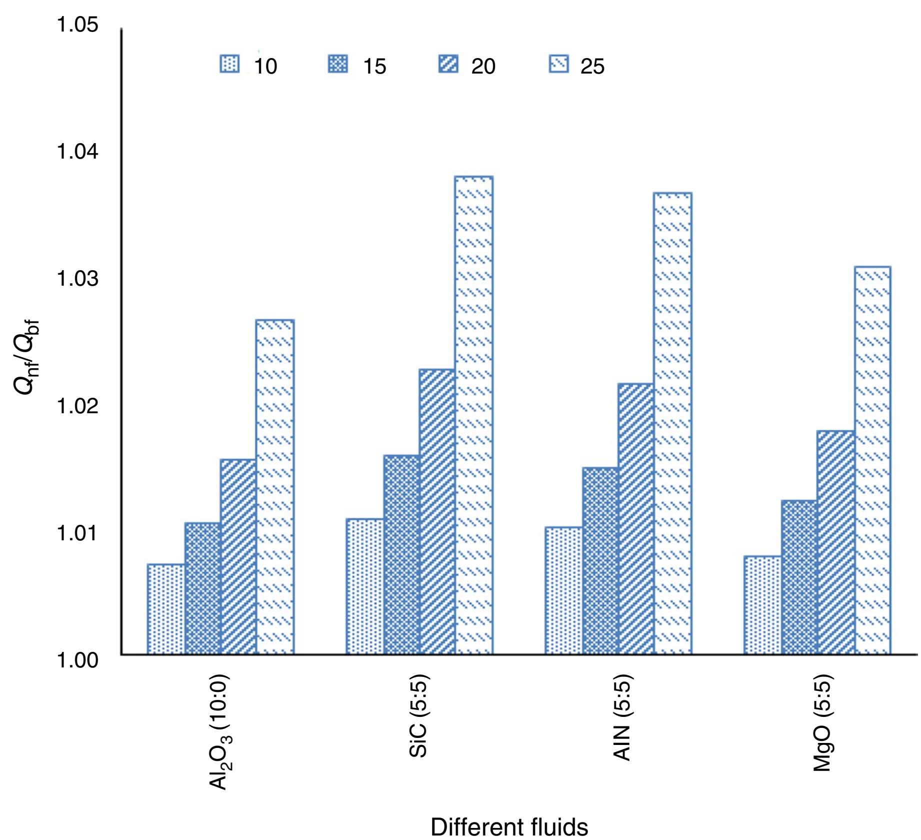

Fig. 11 Change in heat transfer rate with inlet temperature

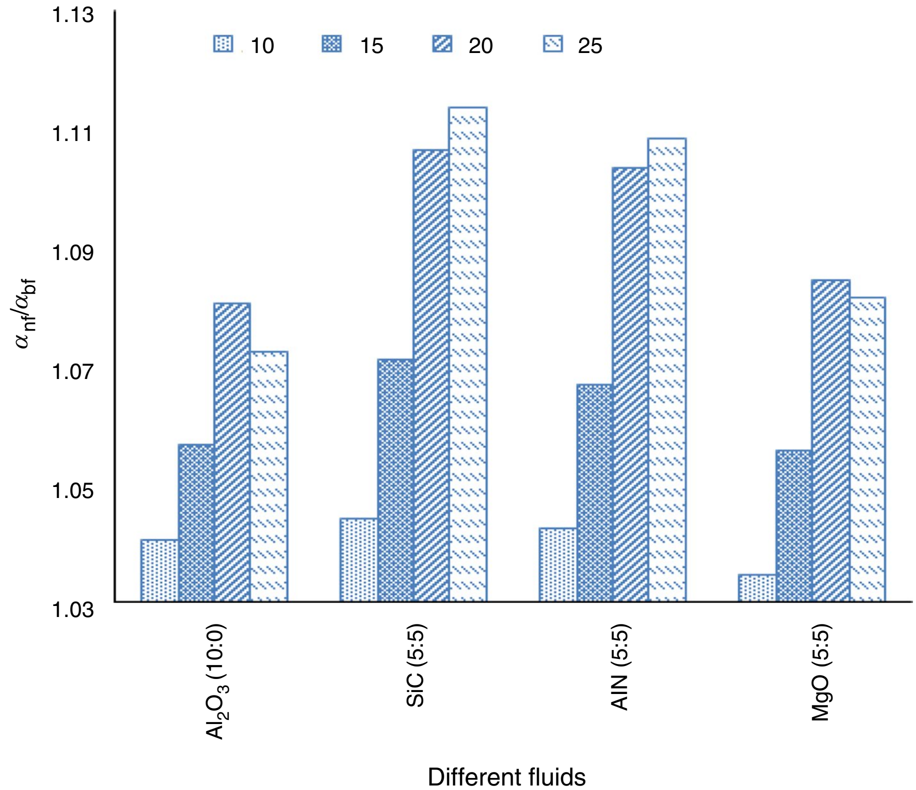

Fig. 12 Change in heat transfer coefficient with inlet temperature

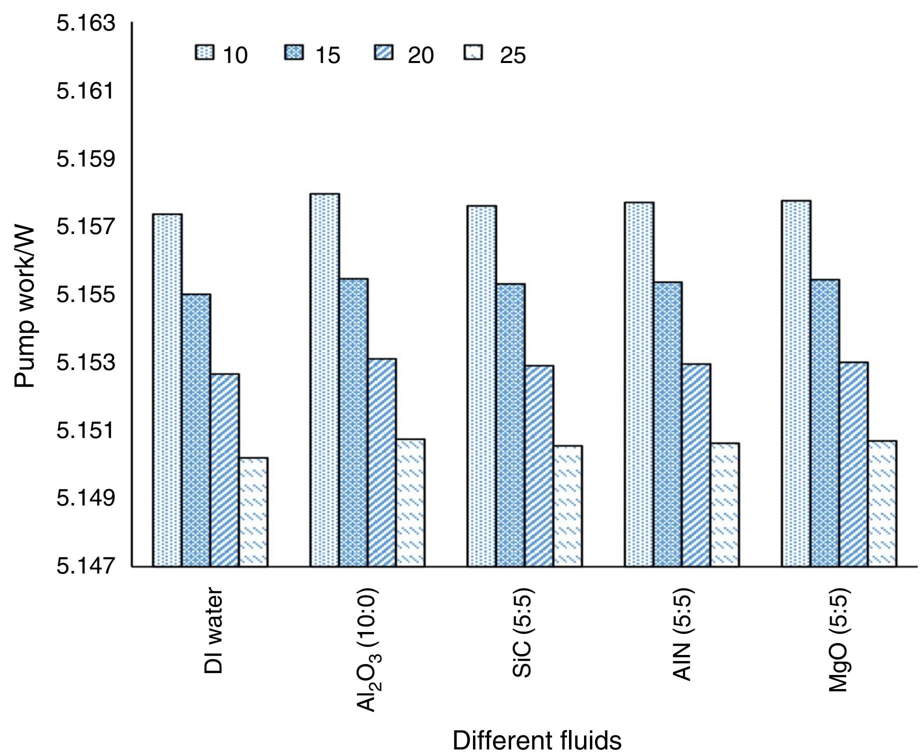

Fig. 13 Change in pump work with inlet temperature

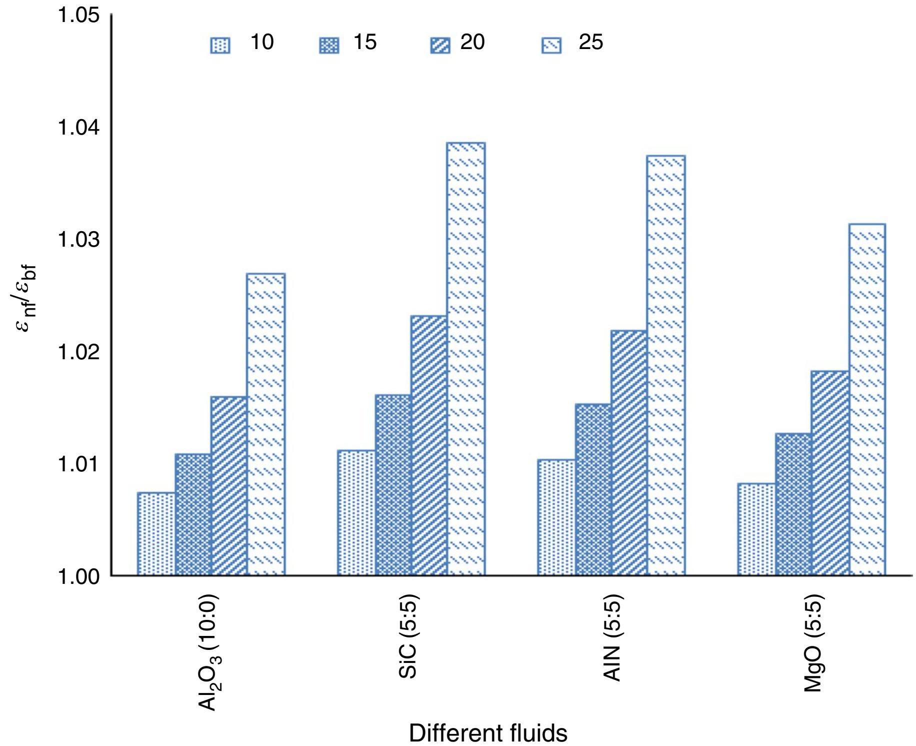

Fig. 14 Change in effectiveness with inlet temperature

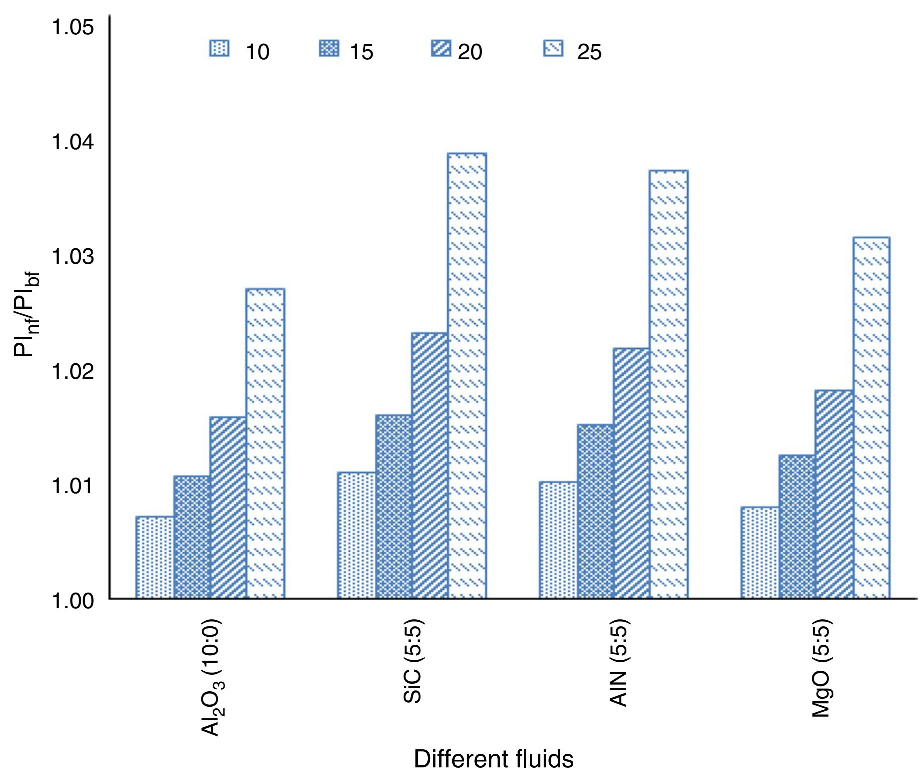

Fig. 15 Change in performance index with inlet temperature

because the ratio of rise in heat transfer rate to rise in pump work is more. SiC (5:5) hybrid nanofluids were found to be more effective in studied cases. However, as the nanoparticles are costlier, they are unable to find their way into the industrial applications at present scenario. So, a lower concentration of nanoparticles should be used to get an earlier payback period [44]. The work was carried out keeping in mind the future scope and technology because hybrid nanofluids are one of the futuristic technologies. One has to work in the area of innovative nanoparticle manufacturing technology to reduce its cost and make nanoparticles in use and improve the thermal performance of plate heat exchangers.

Conclusions

This study experimentally tested the different energy performances of various Al_2O_3–DI water HyNfs in counter-flow-type PHE. This work was carried out for a concentration of 0.01 v% at an equal particle ratio. The coolant flow rate and operating temperatures were varied from 2.0 to 4.0 lpm and 10 to 25 °C, respectively. The low concentration was chosen to decrease the cost of the fluid [38]. The conclusions made from the results and discussion are as follows:

- The heat transfer coefficient augments with the flow rate, inlet temperature, and nanoparticle addition. It rises to 11.7% for silicon carbide/alumina/water hybrid nanofluid.
- The increase in pumping work with the addition of nanoparticles is negligible (0.25%).
- Heat transfer augments with the flow rate and the addition of nanoparticles. It rises to 3.8% for SiC–Al_2O_3 hybrid nanofluid.
- The effectiveness and performance index of heat exchangers increase by about 3.9%.
- Hybrid nanofluids can be a better coolant in plate heat exchangers for sub-ambient temperature applications.
- Hybrid nanofluids can find industrial applications if their cost can be reduced.
- Correlation for predicting the Nusselt number (Eq. 9) has been developed for DI water under the present case parameters.

Findings from this investigation can be used for a better selection of working fluid in the heat exchangers to overcome the energy crisis. In the future, an attempt will be made to propose a generalized correlation for predicting the Nusselt number. Also, the research will be done to reduce the manufacturing cost of the nanoparticles.

Acknowledgements Not applicable.

Authors' contributions The author has done all the necessary work required. There is no contribution of anyone in this regard.

Funding The author declares that no funds, grants, or other support were received during the preparation of this manuscript.

Data availability This is the authors' original data and has not been taken from anywhere. Also, neither was submitted anywhere for publication.

Declarations

Conflict of interest The manuscript has not been previously published, is not currently submitted for review to any other journal, and will not be submitted elsewhere before the decision is made. As this manuscript contains a single author, there is no conflict of interest between the authors and any other person.

Ethics approval Not applicable.

Consent to participate Not applicable.

Consent for publication The author is ready to publish work in this journal.

References

1. Kumar V, Tiwari AK, Ghosh SK. Application of nanofluids in plate heat exchanger: a review. Energy Convers Manag. 2015;105:1017–36.
2. Zheng D, Wang J, Chen Z, Baleta J, Sundén B. Performance analysis of a plate heat exchanger using various nanofluids. Int J Heat Mass Transf. 2020;158:119993.
3. Barzegarian R, Moraveji MK, Aloueyan A. Experimental investigation on heat transfer characteristics and pressure drop of BPHE (brazed plate heat exchanger) using TiO_2–water nanofluid. Exp Therm Fluid Sci. 2016;74:11–8.
4. Göltaş M, Gürel B, Keçebaş A, Akkaya VR, Güler OV, Kurtuluş K, Gürbüz EY. Thermo-hydraulic performance improvement with nanofluids of a fish-gill-inspired plate heat exchanger. Energy. 2022;253:124207.
5. Singh G, Sarao TP. Experimental analysis of heat transfer and friction factor in plate heat exchanger with different orientations using Al_2O_3 nanofluids. Int J Eng. 2016;29(10):1450–8.
6. Peker G, et al. Investigation of the effect of nanofluids on heat transfer enhancement by using parallel and vertical springs in a plate heat exchanger. Heat Mass Transf. 2022. https://doi.org/10.1007/s00231-022-03326-8.
7. Çuhadaroğlu B, Hacisalihoğlu MS. An experimental study on the performance of water-based CuO nanofluids in a plate heat exchanger. Int Commun Heat Mass Transf. 2022;137:106255.
8. Peker G, Yıldız C, Çakmak G, Bilgiç Y, Yıldız A. Thermal performance of new type plate heat exchanger with spring turbulence generator using nanofluid flow. Exp Heat Transf. 2022. https://doi.org/10.1080/08916152.2022.2081886.
9. Behrangzade A, Heyhat MM. The effect of using nano-silver dispersed water based nanofluid as a passive method for energy efficiency enhancement in a plate heat exchanger. Appl Therm Eng. 2016;102:311–7.
10. Sarafraz MM, Hormozi F. Heat transfer, pressure drop and fouling studies of multi-walled carbon nanotube nanofluids inside a plate heat exchanger. Exp Therm Fluid Sci. 2016;72:1–11.

11. Sun B, Peng C, Zuo R, Yang D, Li H. Investigation on the flow and convective heat transfer characteristics of nanofluids in the plate heat exchanger. Exp Therm Fluid Sci. 2016;76:75–86.
12. Kumar V, Tiwari AK, Ghosh SK. Effect of chevron angle on heat transfer performance in plate heat exchanger using ZnO/water nanofluid. Energy Convers Manag. 2016;118:142–54.
13. Jassim EI, Ahmed F. Assessment of nanofluid on the performance and energy-environment interaction of plate-type-heat exchanger. Therm Sci Eng Prog. 2021;25:100988.
14. Sheikholeslami M. Numerical investigation for concentrated photovoltaic solar system in existence of paraffin equipped with MWCNT nanoparticles. Sustain Cities Soc. 2023;99:104901.
15. Sheikholeslami M, Khalili Z, Scardi P, Ataollahi N. Environmental and energy assessment of photovoltaic-thermal system combined with a reflector supported by nanofluid filter and a sustainable thermoelectric generator. J Clean Prod. 2024;438:140659.
16. Sheikholeslami M, Khalili Z. Simulation for impact of nanofluid spectral splitter on efficiency of concentrated solar photovoltaic thermal system. Sustain Cities Soc. 2024;101:105139.
17. Sheikholeslami M, Khalili Z. Solar photovoltaic-thermal system with novel design of tube containing eco-friendly nanofluid. Renew Energy. 2024;222:119862.
18. Sheikholeslami M, Khalili Z. Environmental and energy analysis for photovoltaic-thermoelectric solar unit in existence of nanofluid cooling reporting CO_2 emission reduction. J Taiwan Inst Chem Eng. 2024;156:105341.
19. Pandey SD, Nema VK. Experimental analysis of heat transfer and friction factor of nanofluid as a coolant in a corrugated plate heat exchanger. Exp Therm Fluid Sci. 2012;38:248–56.
20. Javadi FS, Sadeghipour S, Saidur R, BoroumandJazi G, Rahmati B, Elias MM, Sohel MR. The effects of nanofluid on thermophysical properties and heat transfer characteristics of a plate heat exchanger. Int Commun Heat Mass Transf. 2013;44:58–63.
21. Abou Elmaaty TM, Kabeel AE, Mahgoub M. Corrugated plate heat exchanger review. Renew Sustain Energy Rev. 2017;70:852–60.
22. Mansoury D, Doshmanziari FI, Kiani A, Chamkha AJ, Sharifpur M. Heat transfer and flow characteristics of Al_2O_3/water nanofluid in various heat exchangers: experiments on counter flow. Heat Transf Eng. 2019;41:220–34.
23. Sarkar J, Ghosh P, Adil A. A review on hybrid nanofluids: recent research, development and applications. Renew Sustain Energy Rev. 2015;43:164–77.
24. Huminic G, Huminic A. Hybrid nanofluids for heat transfer applications: a state-of the-art review. Int J Heat Mass Transf. 2018;125:82–103.
25. Babar H, Ali HM. Towards hybrid nanofluids: preparation, thermophysical properties, applications, and challenges. J Mol Liq. 2019;281:598–633.
26. Zayed ME, Zhao J, Du Y, Kabeel AE, Shalaby SM. Factors affecting the thermal performance of the plate solar collector using nanofluids: a review. Sol Energy. 2019;182:382–96.
27. Bhattad B, Rao BN, Atgur V, Veza I, Zamri MFMA, Fattah IMR. Thermal performance evaluation of plate-type heat exchanger with alumina–titania hybrid suspensions. Fluids. 2023;8(4):120.
28. Bhattad A, Atgur V, Rao BN, Banapurmath NR, Khan TMY, Vadlamudi C, Krishnappa S, Sajjan AM, Shankara RP, Ayachit NH. Review on mono and hybrid nanofluids: preparation, properties, investigation, and applications in IC engines and heat transfer. Energies. 2023;16(7):3189.
29. Huang D, Wu Z, Sunden B. Effects of hybrid nanofluid mixture in plate heat exchangers. Exp Therm Fluid Sci. 2016;72:190–6.
30. Kumar V, Tiwari AK, Ghosh SK. Effect of variable spacing on performance of plate heat exchanger using nanofluids. Energy. 2016;114:1107–19.
31. Kumar V, Tiwari AK, Ghosh SK. Exergy analysis of hybrid nanofluids with optimum concentration in a plate heat exchanger. Mater Res Express. 2018;5:065022.
32. Kumar D, Tiwari AK. CFD simulation of plate heat exchanger using hybrid nanofluid. Int J Mech Eng Technol. 2018;9(9):1411–8.
33. Bhattad A, Sarkar J, Ghosh P. Discrete phase numerical model and experimental study of hybrid nanofluid heat transfer and pressure drop in plate heat exchanger. Int Commun Heat Mass Transf. 2018;91:262–73.
34. Bhattad A, Sarkar J, Ghosh P. Experimentation on effect of particle ratio on hydrothermal performance of plate heat exchanger using hybrid nanofluid. Appl Therm Eng. 2019;162:114309.
35. Bhattad A, Sarkar J, Ghosh P. Hydrothermal performance of different alumina hybrid nanofluid types in plate heat exchanger. J Therm Anal Calorim. 2020;139:3777–87.
36. Sokhal GS, Dhindsa GS, Jakhar A, Malhi GS, Tonk R. Role of hybrid nanofluids on the performance of the plate heat exchanger: experimental study. Mater Today Proc. 2022;68(4):962–7.
37. Bhattad A, Sarkar J, Ghosh P. Exergetic analysis of plate evaporator using hybrid nanofluids as secondary refrigerant for low temperature applications. Int J Exergy. 2017;24(1):1–20.
38. Bhattad A, Sarkar J, Ghosh P. Energy–economic analysis of plate evaporator using brine based hybrid nanofluids as secondary refrigerant. Int J Air-Cond Refrig. 2018;26(1):1850003.
39. Bhattad A, Sarkar J, Ghosh P. Energetic and exergetic performances of plate heat exchanger using brine based hybrid nanofluid for milk chilling application. Heat Transf Eng. 2020;41(6–7):522–35.
40. Goodarzi M, et al. Investigation of heat transfer and pressure drop of a counterflow corrugated plate heat exchanger using MWCNT based nanofluids. Int Commun Heat Mass Transf. 2015;66:172–9.
41. Huang D, Wu Z, Sunden B. Pressure drop and convective heat transfer of Al_2O_3/water and MWCNT/water nanofluids in a chevron plate heat exchanger. Int J Heat Mass Transf. 2015;89:620–6.
42. Pantzali MN, Kanaris AG, Antoniadis KD, Mouza AA, Paras SV. Effect of nanofluids on the performance of a miniature plate heat exchanger with modulated surface. Int J Heat Fluid Flow. 2009;30:691–9.
43. Kakac S, Liu H. Heat exchangers: selection, rating and thermal design. 2nd ed. Florida, USA: CRC Press LLC; 2002.
44. Singh SK, Sarkar J. Energy, exergy and economic assessments of shell and tube condenser using hybrid nanofluid as coolant. Int Commun Heat Mass Transf. 2018;98:41–8.